1 Si/Si:Er multinanolayers

Nihil volitum quin praecognitum.
Nihil cognitum quin praevolitum.

In this chapter an in-depth study of the optical properties of silicon doped with erbium ions is presented. The first section 1.1 deals with fundamental aspects of the energy transfer processes between the host and the optically active material, *i.e.* the excitation mechanisms that result in the optical excitation of Er^{3+}; experimental evidence is provided to prove the role of the Er-related donor in its excitation via the Si host, and a new excitation mechanism is proposed and demonstrated. The sample chosen for this study consists on a Si/Si:Er^{3+} multinanolayer structure—details are given further in the chapter. Previous work has shown that a single type of Er center is predominantly formed in such a system [6], simplifying thus the realization of experiments that will provide a comprehensive understanding of the energy transfer process: a single Er center would presumably form a single Er-related donor level.

Whereas the first section 1.1 of this chapter focuses on the basic mechanisms underlying optical excitation of Er-doped crystalline silicon (c-Si:Er^{3+}) and involves cryogenic temperatures and experiments at a free electron laser (FEL) users facility, the second section 1.2 proves the potential of the Si/Si:Er^{3+} multinanolayer system for *real-life* applications. Here, a fully CMOS compatible electro-optical converter with a memory function is presented and its functionality demonstrated. Following previous work on the observed memory effect of c-Si:Er^{3+} in photoluminescence [7, 8], we demonstrate full *write-read-erase* electrically driven functionality realized outside of cryogenic temperatures. Finally, an erbium-doped silicon based cross point memory array is proposed as a possible future memory photonic device.

1.1 Donor-state enabling Er-related luminescence in silicon

A direct link between formation of an Er-related donor gap state and the 1.5 μm emission of Er in Si will be conclusively established in this section. The experiment was performed on Si/Si:Er nanolayers where a single type of Er optical center dominates. We show that the Er emission can be resonantly induced by direct pumping into the bound exciton state of the identified donor. Using two-color spectroscopy with a free-electron laser, the ionization energy of the donor state enabling Er excitation was determined as $E_D \approx 218$ meV. Quenching of the Er-related emission upon ionization of the donor is also demonstrated.

1.1.1 Introduction

Doping with Er is possibly the most investigated way for improving photonic properties of crystalline silicon. Nevertheless, the low level of optical activity of Er^{3+} and thermal quenching of emission intensity—two major obstacles precluding application of Si:Er for practical devices—have not been resolved. Moreover, the physical basis of these limitations is not fully understood. This justifies further research in fundamental aspects of energy transfer mechanisms governing excitation and de-excitation processes of Er^{3+} ions embedded in a c-Si matrix. Among different issues related to this problem, the proposed formation of a gap state mediating energy flow between extended effective-mass-like shallow levels of the host and localized 4f-electron states of Er^{3+} is of profound importance. Thus far only indirect evidence in support of the Er-related donor level has been derived from thermal quenching of Er luminescence [9] and deep-level transient spectroscopy (DLTS) measurements [10,11], where ionization energy E_D values between 150 and 250 meV have been reported. These measurements, however, are not able to discriminate between optically active—*i.e.*, taking part in the photoluminescence process—and non-active fractions of Er dopants. Consequently, the often postulated link between formation of a donor level and optical activity of Er^{3+} is not supported by these experiments, that naturally reflect properties of the majority of Er dopants, which do not take part in light emission. In addition, the formation of an Er-related donor level in Si has never been justified by theoretical modelling; this in contrast to Yb^{3+} in InP [12]. Therefore it is possible that the donor level observed in c-Si:Er is induced by Er doping but bears no microscopic relation to optical activity of Er^{3+}. One possibility could be formation of the so called *thermal donor* [13], since Er is known to promote oxygen aggregation which leads to generation of thermal donors.

As can be concluded from the above, the identification of a gap state mediating the energy transfer to (and from) the Er^{3+} ion, and in this way controlling its optical activity in c-Si, remains open. At the same time, this issue is of paramount importance, both fundamental (for understanding of energy transfer processes) and practical (for excitation engineering towards improvement of thermal stability of emission). In the present study we resolve this long-standing problem: using complementary information obtained by excitation and two-color spectroscopies, we identify a specific donor state and establish its unambiguous link with the 1.5 μm emission in c-Si:Er.

1.1.2 Experiment

Photoluminescence (PL) excitation spectroscopy (PLE) was performed at T = 10 K under pulsed excitation with an optical parametric oscillator (OPO), tunable in the near-infrared range, close to the band gap of c-Si. The two-color measurements were performed at the free-electron laser users facility FELIX in Nieuwegein, the Netherlands. The third harmonic of the FEL was used to enable a probe wavelength in the spectral range between 2.55 and 8.27 μm (150 to 485 meV). For primary excitation, the second harmonic of a Nd:YAG laser (532 nm) was applied. The duration of the Nd:YAG pulse was shorter than 100 ps, while the full width at half maximum (FWHM) of the total FEL macro-pulse was about 5 μs. The delay time Δt between the primary (Nd:YAG) and secondary (FEL) pulse could be tuned at will. The measurements were taken at T = 4.2 K using a gas-flow cryostat. PL spectra were resolved with a TRIAX 320 spectrometer and detected with an InGaAs photomultiplier tube.

Sample

The study was conducted on a Si/Si:Er multinanolayer structure grown by sublimation MBE technique, comprising 400 alternating Si and Si:Er layers on a Cz-Si substrate. As discussed before [6], the Er^{3+} ions in this sample form predominantly only a single type of center, whose PL is characterized by homogeneous and ultra-small linewidth of $\Delta E < 10$ μeV. The low temperature PL spectrum of the investigated sample—see *e.g.* [6]—features a series of very sharp lines related to the $^4I_{13/2} \rightarrow ^4I_{15/2}$ transition of the Er^{3+} ion, with the main emission at 1538 nm. This system is particularly suitable for the investigation of the Er-related level in the excitation process. It can be expected that a single type of optical center will create a single level in the Si band gap, thus considerably simplifying the experiment.

1.1.3 Results and Discussion

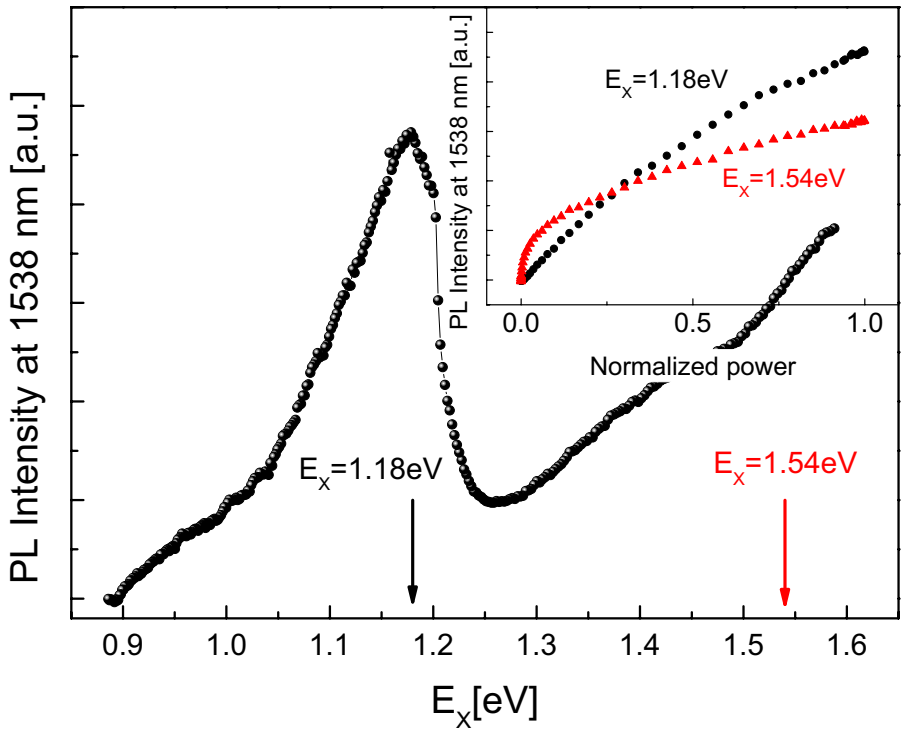

Figure 1.1: *PLE spectrum of the 1.5 μm Er-related emission. For two excitation wavelengths indicated with arrows, normalized power dependence of the PL intensity is given in the inset.*

In Fig. 1.1, the PLE spectrum of the Er-related emission measured in the investigated structure for excitation energy E_X close to the band gap of c-Si is presented. As can be seen, in addition to the usually observed contribution produced by (the onset of) the band-to-band excitation, also a resonant feature, peaking at the energy around $E_X = E_R \approx 1.18$ eV is clearly visible. We propose to identify this with a different excitation channel appearing in this energy range. Such a hypothesis is directly supported by PL intensity power dependence, shown in the inset, for the two photon energies indicated with arrows. While the data obtained for the higher energy value of $E_X = 1.54$ eV exhibit the saturating behavior characteristic of the band-to-band excitation mode [14], the dependence for $E_X = E_R \approx 1.18$ eV has a strong linear component superimposed on this saturating background. Such a linear dependence is expected for "direct" pumping. For Er in c-Si a resonant excitation could indeed take place via a bound exciton state induced by the long-sought Er-related donor discussed earlier. In that case, the energy E_R

required for this resonant pumping would be given by:

$$E_R \approx E_G - E_{FEX} + E_{LO} - E_{BE}, \tag{1.1}$$

where E_G is the c-Si band gap energy $E_G = 1.17$ eV, $E_{FEX} = 15$ meV is the exciton formation energy, E_{LO} is the energy of the lattice phonon whose participation in the excitation process is necessary in view of the indirect band gap of c-Si, and E_{BE} is the exciton-donor binding energy. Using the $E_R \approx 1.18$ eV value derived from the PLE spectrum given in Fig. 1.1, we can estimate the exciton binding energy as $E_{BE} \approx 30$ meV. Since exciton binding and donor ionization energies of a donor are mutually related—for effective-mass donors $E_{BE} \approx 10\% E_D$ is commonly found—, this implies that the relevant donor state involved in the postulated resonant excitation of Er is relatively deep, with the ionization energy in the range of 200-300 meV.

PL quenching

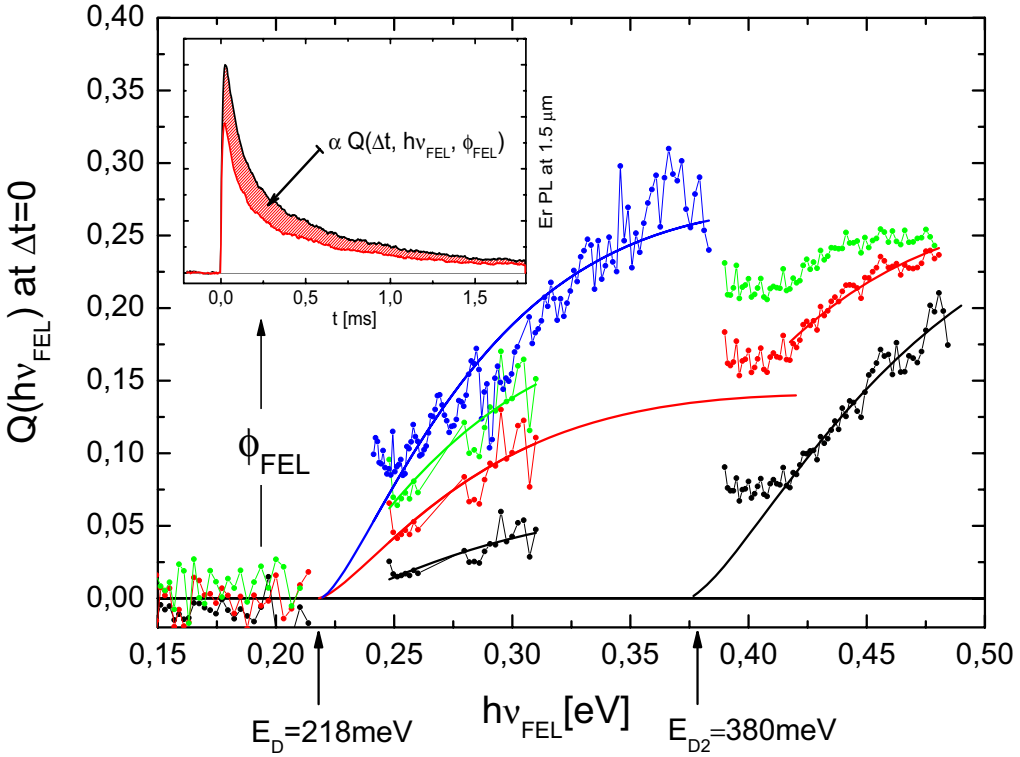

Figure 1.2: *FEL wavelength dependence of the induced quenching ratio of Er-related PL at 1.5 µm, for several flux settings of the FEL. Solid lines correspond to simulations with Eq. 1.3. In the inset: illustration of the FEL-induced quenching of Er-related PL.*

Direct identification of this donor state governing the optical activity of Er in c-Si and enabling its excitation has been obtained by two-color spectroscopy

in the visible and the mid-infrared (MIR) regions. In the past, this powerful experimental technique [8] has been successfully applied for investigation of excitation mechanisms in rare-earth-doped matrices [15–17], spin relaxation in semiconductors [18], and excited states of atomic clusters [19]. In these experiments one monitors the PL of the system emitted after band-to-band excitation with the primary pulse, which is then altered by the secondary MIR beam (FEL). In the current case, we have observed that the Er-related PL is quenched upon application of a FEL pulse with a sufficiently large photon quantum energy. This is illustrated in the inset to Fig. 1.2, which shows the change of the PL transient induced by the MIR pulse. Amplitude of the relative quench remains independent of temperature, up to at least 70 K, thus indicating a deeper character of the levels involved in the process [8, 20, 21]. Detailed investigations revealed that the magnitude of quenching depends on the timing of the FEL with respect to the band-to-band excitation Δt, and on the quantum energy $h\nu_{FEL}$ and the flux ϕ_{FEL} of the MIR photons. In order to quantify these effects, we define the quench ratio as

$$Q(\Delta t, h\nu_{FEL}, \phi_{FEL}) = \frac{\Delta I}{I} = 1 - \frac{\int_{\Delta t}^{\infty} E^*_{FEL}(t)dt}{\int_{\Delta t}^{\infty} E^*_{noFEL}(t)dt}, \tag{1.2}$$

where I stands for the time-integrated PL intensity, from the moment when the MIR pulse is fired, and E^*_{FEL} and E^*_{noFEL} are the PL signals observed with and without the FEL pulse, respectively. $Q = 1$ corresponds to the total quench of the PL signal. Fig. 1.2 shows the wavelength dependence of PL quench for several flux values. As can be seen, PL quenching is observed for the MIR photon energy $h\nu_{FEL} \geq 250$ meV, but not in the region $h\nu_{FEL} \leq 210$ meV. We conclude that the quenching effect appears once the photon quantum energy exceeds a certain threshold value located between 210 and 250 meV, and saturates at a higher photon flux—see Fig. 1.3—with the maximum signal reduction of $Q \approx 0.35$. Fig. 1.4 shows the quench ratio as a function of the time delay Δt. As can be seen, the quenching does not take place when the FEL is fired before the pump, gradually increases as the two pulses overlap (-8 μs $\leq \Delta$t ≤ 0 μs), attains maximum for Δt ≈ 0 μs—see the detailed kinetics in the inset—and then slowly, on the time scale of $\tau_d \approx 300$ μs, reduces towards an equilibrium value of $Q_{eq} \approx 10\%$. This observation excludes heating as a possible explanation for the reduction of PL, since this has a relaxation time of an order of milliseconds and therefore PL quenching should take place also for FEL pulses applied before the Nd:YAG. We conclude that application of FEL induces an additional, non-radiative de-excitation of Er^{3+} ions. One possible candidate for such a process could be cooperative up-conversion, well-known from Er-doped glasses. In this case energy is transferred between two excited

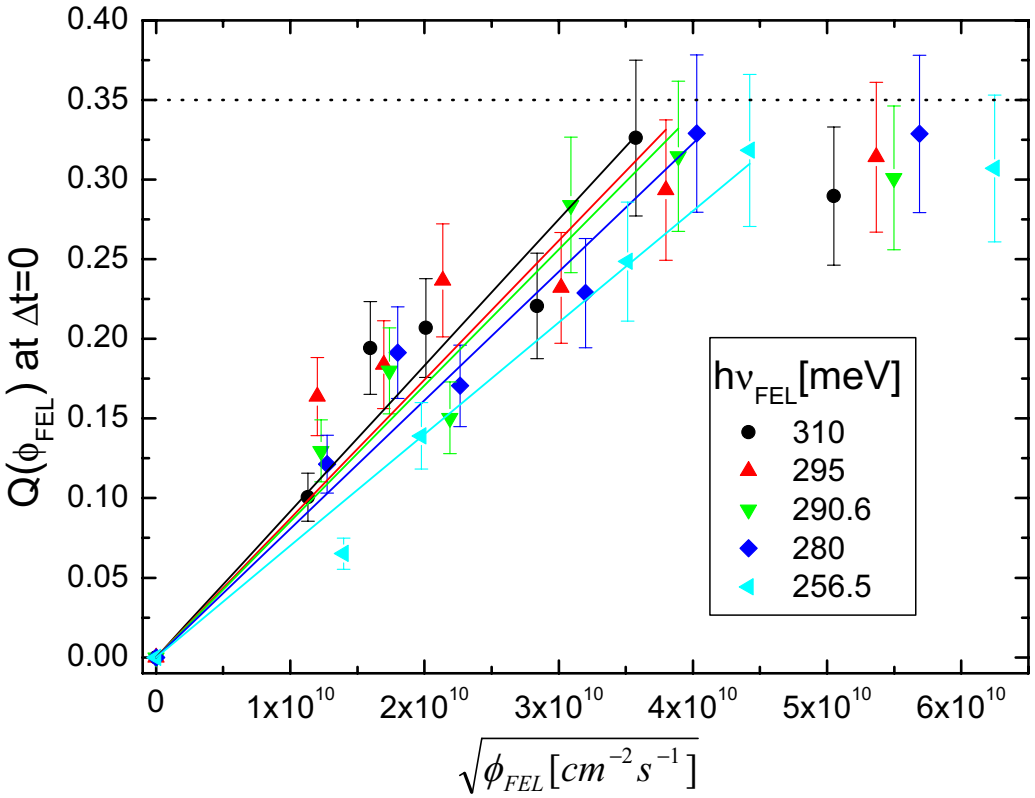

Figure 1.3: *Quenching ratio as a function of the square root of the FEL photon flux for* $h\nu_{FEL}$ *= 310, 295, 290.6, 280, and 256.5 meV,* $T = 4.2$ *K,* $\Delta t = 0$*. Linear dependence is shown for low flux values; the saturation level is indicated with the dotted line at* Q *= 0.35.*

Er^{3+} ions. Effectively, this means that one excitation is lost. However the up-conversion process depends only on the average distance between ions and on the medium, and can not be influenced by photons from the FEL. This rules out up-conversion as a possible mechanism of the FEL-induced PL quenching.

A prominent non-radiative recombination processes pertinent to Er-doped c-Si is the excitation reversal ("back-transfer"). It has been identified as the main reason for reduction of Er^{3+} luminescence at elevated temperatures and involves creation of an electron-hole pair at the Er-related level at the expense of Er^{3+} de-excitation. At higher temperatures, the additional energy required for this process is provided by multi-phonon absorption. For InP:Yb, it was shown that the "back-transfer" can also be induced by intense FEL illumination. In that case a step-like dependence on photon energy and a linear dependence on photon flux, leading to complete quenching of the emission, have been observed [17]. This is clearly different in the present case, where a pronounced wavelength dependence and also saturation of the quench

ratio are measured. We note further that when we assume that the resonant feature of Fig. 1.1 represents the Er-related BE state, then the minimum activation energy necessary for the back-transfer can be estimated as $E_{bt} \geq E_R - E_{PL} \approx 1180 - 800$ meV $= 380$ meV. In contrast to that, data in Fig. 1.2 show PL quench already at much smaller energies. Taken together, the evidence at hand argues against identification of the observed PL quenching with the "back-transfer". Also the afore mentioned thermal stability of the observed quenching points against the "back-transfer", as this process should enhance upon temperature increase—to this end we point out that complete PL quench is indeed observed at higher temperatures.

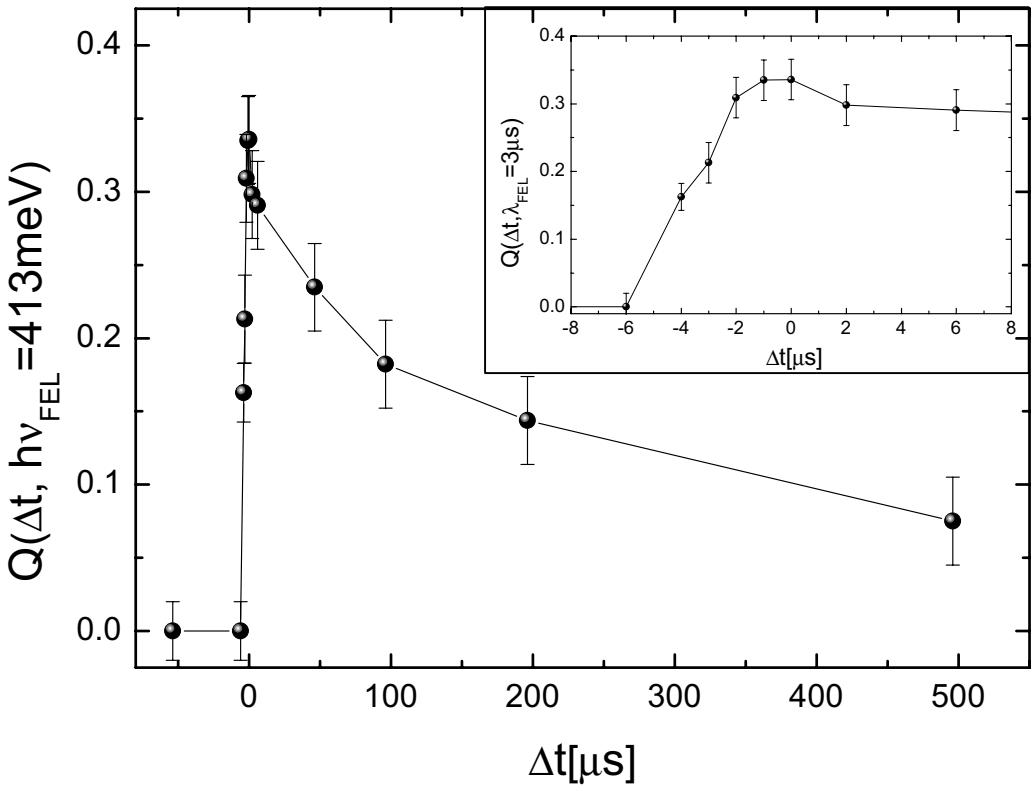

Figure 1.4: *Quenching ratio as a function of mutual delay of pump and probe pulses Δt, for $h\nu_{FEL} = 413$ meV. In the inset: detailed behavior for the region of overlap between the pump and the FEL pulses.*

In the past, also Auger process has been found to hamper PL process of Er in c-Si: a carrier in the conduction or valence band can absorb the energy of an excited Er^{3+} ion, leading to PL quenching [22]. Auger quenching can be induced with the FEL by optical ionization of trap states [21]. In that case, the quench rate is proportional to the concentration of carriers liberated by the FEL pulse. Assuming that an equilibrium carrier concentration is

maintained during FEL illumination, the PL quenching should increase with the square root of photon flux [14] towards saturation determined by full ionization of relevant traps. As evidenced by Fig. 1.3, this characteristic square root dependence is indeed observed in the experiment for small photon fluxes. On the other hand, the quench should increase (practically linearly) with the exposure time of excited Er population to free carrier concentration, *i.e.* with the "effective" duration of the FEL pulse, again in agreement with the experiment—see Fig. 1.4. (In view of the relatively slow character of processes considered in this study, the "macropulseï¿½ of FEL, featuring a 1 GHz train of picosecond pulses, can be seen as being practically "rectangularï¿½, with picosecond rise and decay slopes.) We also note that following the full overlap of the two pulses, a small decrease of the quench takes place upon further increase of the delay time. It is plausible to attribute this gradual reduction to decay of (non-equilibrium) population of traps involved in the Auger process. This effect additionally supports the proposed microscopic identification of the PL quenching being an Auger process rather than the "back-transfer", which should be time-independent. Finally, it is only fair to point out that the energy (back-)transfer process in Si:Er is significantly more complex than in direct band gap materials; therefore we cannot rule out that it indeed contributes to the observed quenching.

Since for the fixed duration of the FEL pulse, the Auger effect should saturate at a level determined by trap concentration, then the quenching saturation level can be used to estimate this concentration. Taking the maximum quench to be 35% of the original signal—Fig. 1.3—and the FEL pulse FWHM as 5 μs, and using the frequently quoted value of the Auger coefficient for free electrons of $C_A \approx 10^{-13} - 10^{-12}$ cm^{3}s^{-1} [22], we arrive at a trap concentration of $10^{17} - 10^{18}$ cm^{-3}. This concentration is much higher than the donor/acceptor doping level of the matrix and can only be compared to the concentration of Er-related donors found in an oxygen-rich material [23].

Following our microscopic interpretation of the quenching mechanism, its wavelength dependence should reflect photoionization spectrum of traps releasing carriers taking part in the Auger energy transfer. It has been shown [24] that the ionization cross section for traps can be described by:

$$\sigma(h\upsilon) \propto \frac{(h\upsilon - E_D)^{3/2}}{h\upsilon^{3+2\gamma}}, \tag{1.3}$$

with $h\upsilon$ and E_D corresponding to the quantum energy of the ionizing radiation and the ionization energy of the trap, respectively. The parameter γ depends on the specific form of the binding potential, being $\gamma = 0$ for δ-like potentials and $\gamma = 1$ for Coulomb potentials. Since $Q \propto \sigma(h\upsilon)$ then we can fit the data in Fig. 1.2 with Eq. 1.3. In this way we find the thermal ionization energy

of the involved level as $E_D = 218 \pm 15$ meV. Note that only the low FEL flux data are used for fitting, in order to minimize saturation effects. The best fit has been obtained for a localized potential, with $\gamma \approx 0$. We recall that $E_D \approx 218$ meV is similar to the trap level found in Si:Er by DLTS [11]. Therefore, it appears plausible that the FEL ionizes electrons from the donor level associated with Er^{3+}, the same as identified earlier from the PLE data. Further, it appears that in the high photon energy range, another deeper trap, with ionization energy in 350 - 450 meV range, contributes to the free carrier density.

1.1.4 Conclusions

We conclude that the results obtained in two-color and excitation spectroscopy explicitly demonstrate that optical activity of Er in c-Si is related with a gap state. Taking advantage of the preferential formation of a single optically-active Er-related center in sublimation MBE-grown Si/Si:Er multinanolayer structures, we determine the ionization energy of this state as $E_D \approx 218$ meV. We prove that this level provides indeed the gateway for Er^{3+} excitation by demonstrating 1.5 μm emission upon resonant pumping into the bound exciton state of the identified donor. We point out that the relatively large width of the resonant excitation band, exceeding that for bound exciton recombination bands in Si [25], follows directly from the involved physical mechanism. In the current case, the absorption of a photon by a bound exciton is accompanied by a simultaneous excitation of Er^{3+} ion and a transfer of a donor electron into the conduction band. Therefore, the minimum energy E_{Xmin} required for this process is given by the sum of Er excitation (800 meV) and donor ionization (218 meV): $E_{Xmin} \approx 1.020$ eV. This corresponds precisely to the onset of the resonant excitation band, as evidenced by Fig. 1.1, thus supporting the proposed identification.

At the same time, we show that carriers located at the Er-related donor state introduce a channel of effective non-radiative relaxation of excited Er^{3+} ions via Auger process of energy transfer. In this way, new light is shed on the long standing puzzle concerning the physical origin of the low emission intensity from Er-doped c-Si: while formation of the donor state enables Er core excitation, the same donor level opens also an efficient path of non-radiative relaxation. Future research will tell whether these two processes can be separated by careful material engineering. We would also like to point out that the direct "resonant" pumping into the bound exciton state identified here allows for excitation of Er^{3+} while avoiding Auger quenching by free carriers.

1.2 Electro-optical memory effect for 1.5 μm photonics

Silicon photonics is rapidly growing and a number of Si-based active and passive components have recently been shown. Here we demonstrate new functionality of Er-doped silicon: a memory effect in electroluminescence. This finding opens a prospect of necessary and thus far not available component for Si optoelectronics—a fully CMOS compatible electro-optical converter with a memory function—operating in the technologically important 1.5 μm band. When developed and optimized, prospect applications could include optical intra- and inter-chip connectors and volatile flash memory elements.

1.2.1 Introduction

In spite of its natural constraint of a small and indirect band gap, crystalline silicon continues to attract interest as a photonic material. Research is clearly fuelled by prospects of a photonic technology fully compatible with CMOS microelectronics. Photonics would constitute silicon's natural extension toward generating smaller, cheaper and ever faster devices. Somewhat surprisingly, c-Si features some properties of an excellent optical material [26, 27]. In particular, the exceedingly high level of impurity control and surface/interface passivation leads to very long minority carrier lifetimes, as non-radiative recombination can be largely suppressed. As a result of continued effort, efficient room-temperature emission has been demonstrated for a number of structures [28–32]. In a parallel development, the optical properties of Si nanocrystals have been exploited leading to the observation of optical gain [33], optical memory [34], and fabrication of LED's [35]. In a different approach, doping with erbium (Er) has been intensively studied as a convenient way to enhance the photonic properties of Si. For c-Si:Er, some promising optical behavior, such as afterglow effects—typical features of standard optical materials such as phosphors—has been revealed using two-color spectroscopy with a free-electron laser [7, 8]. Here we show that c-Si:Er has come of age by demonstrating full *write-read-erase* optical memory functionality for Si:Er structures grown using sublimation molecular beam epitaxy (SMBE) [36]. The breakthrough here is that this embryonic technology does not rely on the use of free-electron lasers or other exotic optical tools, but is facilitated purely via electroluminescence (EL). These findings open new routes for the development of an optoelectronic converter with memory functions for Si-based photonic circuits operating in the 1.5 μm telecommunication wavelength, and thus ushers in an era of optical memory fully integrable with the CMOS platform.

As c-Si-based microelectronics continues its impressive development, breaking speed and definition limits predicted only a few years ago, there appears a

growing awareness that silicon may also be a basis of future optoelectronic and photonic technology. While several other materials, and most notably III-V compounds, have clearly better optical properties, their processing technologies are less advanced, more expensive and unlikely to ever compete or become compatible with the Si platform. For the practical realization of Si photonics, all the components necessary for light manipulation, *i.e.* generation, modulation, mixing and splitting, storage and detection need to be developed. Moreover, these photonic circuits should preferably operate around a wavelength of $\lambda \approx 1.5$ μm, which coincides with the absorption minimum of glass fibers used for transmission of optical signals. Here, impressive progress has been made in the last few years. In addition to the afore mentioned room temperature Si-based emitters [29–34], an optically pumped Si Raman laser has recently been developed [37–39] and a fast optical modulator with operational frequency of 1 GHz has also been demonstrated [40]. While these achievements bring the development of all-Si photonic circuits [41] closer, a crucial part of the puzzle is still missing: a CMOS compatible electro-optical memory element.

1.2.2 Preliminaries

In the past decade, considerable research effort has been aimed at designing storage devices for use in optoelectronics and photonics. A particularly vigorous activity has concentrated on the development of non-magnetic, all-optical storage media. Most of these investigations have been focused on electron trapping at deep centers and/or structural transformations of centers upon carrier trapping, which promise very high *read/write* data transfer rates [42, 43]. In such an approach, information is written by photoionization of deep traps; this effectively sensitizes the material by generating metastable states that modulate locally its electric and/or optical properties. Information can be retrieved optically by exposing the sensitized areas to a *reading* laser beam. Three-dimensional holographic storage in photorefractive materials is another approach towards optical memory devices making use of the interference pattern in non-linear crystals [44].

Up to now, the storage potential of c-Si:Er has only been shown in fundamental laboratory experiments involving optical pumping at very low temperatures [7]. In this case—see Fig. 1.5—it was demonstrated that Er emission could be excited by a pulse of a free-electron laser operating in the mid-infrared range with $h\nu \ll E_G$, but only if it was applied shortly ($\Delta t \lesssim 100$ ms) after band-to-band excitation of the Si matrix ($h\nu > E_G$). The 1.5 μm emission did not appear if the mid-infrared pulse was not preceded by a band-to-band excitation. This memory effect has been explained in terms of temporary stor-

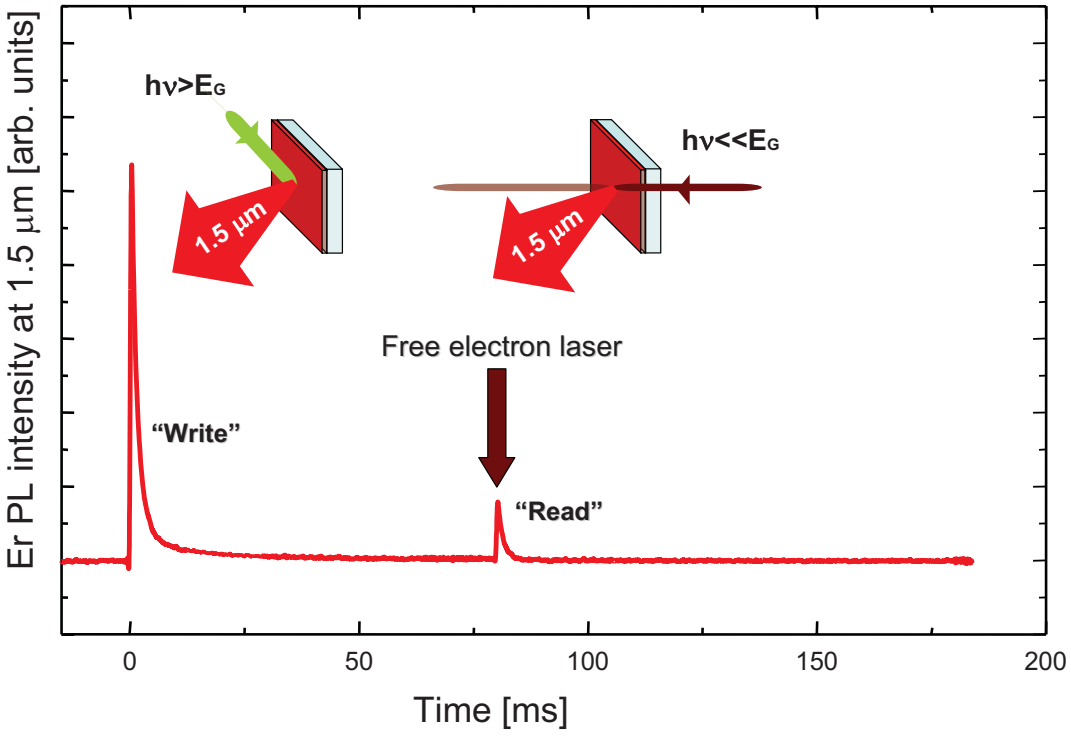

Figure 1.5: *The memory effect in photoluminescence observed for c-Si:Er at low-temperatures (<50 K) in a two color experiment. At time t = 0, a short pulse from a laser (depicted in green) provides band-to-band excitation. This results in filling of the trapping centers (*writing *operation) and an Er-related luminescence signal (at λ = 1.54 μm) with a characteristic decay time of 1 ms. After a delay time, a pulse of mid-infrared radiation from a free-electron laser releases the trapped carriers and thus recovers the stored information (*reading *operation), inducing an Er-related PL signal.*

age of photo-excited carriers at deep traps. Releasing them optically by the mid-infrared laser irradiation—*reading*—, results then in Er^{3+} excitation, but only upon prior exposure of the material to the *writing* laser pulse.

1.2.3 Results

Since this phenomenon of optical memory in Si:Er had been observed only at cryogenic temperatures T $\lesssim$ 50 K and with a free-electron laser as the mid-infrared *reading* beam, it was certainly not relevant for applications. Nevertheless, it indicated that c-Si:Er can be coaxed into having the right kind of optical properties for a Si-based optical storage element for 1.5 μm photonics. Now we are able to take a real step towards commercial exploitation of

these advantageous optical properties, as we present an electrically controlled memory element with optical output. We have succeeded in accomplishing a complete sequence of *writing*, *reading*, and *erasing* operations using electrical pulses of small amplitude, while the optical signal is being emitted in the technologically relevant 1.5 μm band. In comparison to the original concept [7], the operational parameters have been significantly improved. The temperature range has been increased by a factor of 3, to 120 K, and retention times between the *writing* and the *reading* pulses are of the order of seconds. Moreover, there appear to be no fundamental reasons which would prohibit room-temperature operation, as EL of Si:Er under the reverse bias regime is well-known to be thermally stable. Also, a further increase of the retention time should be possible, as a more detailed understanding of the relevant physical processes develops. Fig. 1.6 shows the layer sequence of

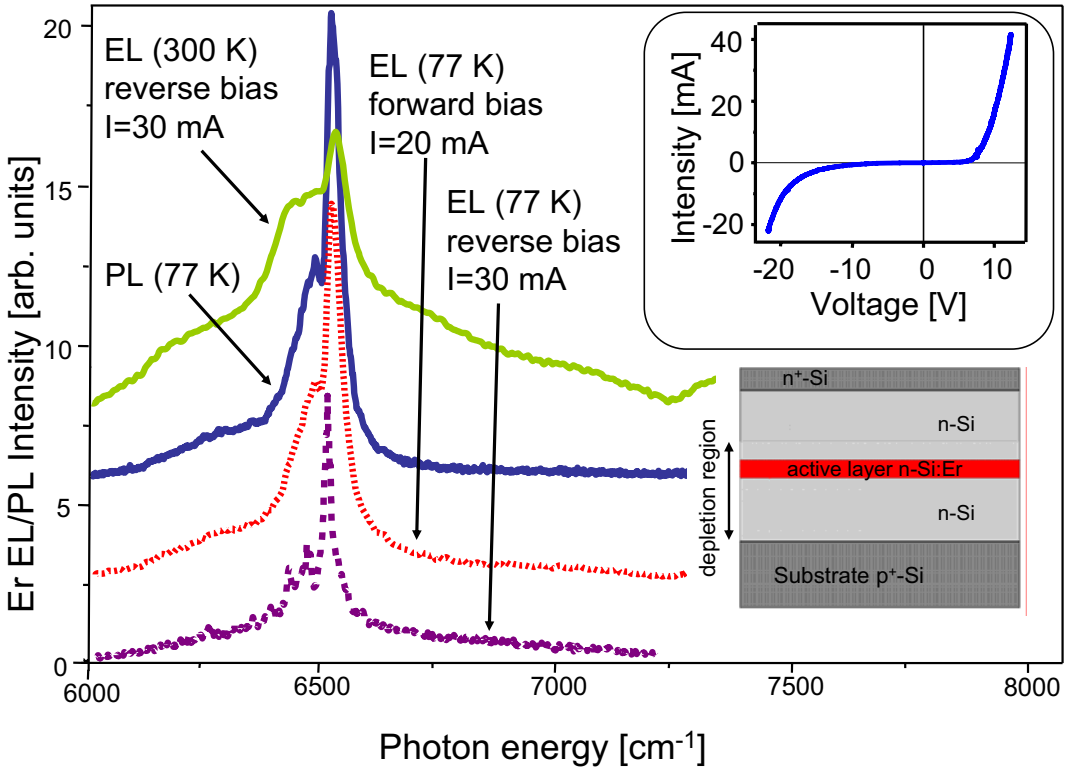

Figure 1.6: *Photo- and electroluminescence spectra of the structure used in the study: the* $\sim$ *1.5 µm band is characteristic of the* ${}^4I_{13/2} \rightarrow {}^4I_{15/2}$ *transition of* Er^{3+} *ions in oxygen-rich Si. The layer sequence of the diode is given in the right-lower corner. As can be seen, the Er-doped active layer is contained within the depletion region (shaded). The upper inset shows current-voltage characteristics of the structure.*

the n^+-Si/n-Si/n-Si:Er/n-Si/p^+-Si electroluminescent memory element. The

structure was grown by the SMBE technique on a p-type (100)-oriented Si substrate with a carrier concentration of p $\approx 10^{17}$ cm^{-3}. It comprises a 1 μm layer of n-type Si with a free carrier concentration of n $\approx 2\times10^{15}$ cm^{-3}, followed by a thin Er-doped active layer of 70 nm thickness, another layer of n-type Si, of 10 μm, and finally an n$^+$ layer with n $\approx 6\times10^{18}$ cm^{-3}. The Er concentration in the active layer is estimated as [Er] $\approx 10^{18}$ cm^{-3}. The diode structure geometry was chosen in such a way that the Er-doped active layer was located within the space charge region. As can be seen from Fig. 1.6, the structure shows intense Er-related $\lambda \approx 1.5$ μm PL and EL under forward bias at low temperatures. Under reverse bias, strong EL was observed up to room temperature. The emission spectra are typical for Er^{3+} ions in a matrix of oxygen-rich Si [45]. The current-voltage characteristic of the structure (at T = 77 K) is also shown as an inset. It exhibits an avalanche-type breakdown for a reverse bias of $U_B \approx$ -(18-20) V. Investigations of the structure

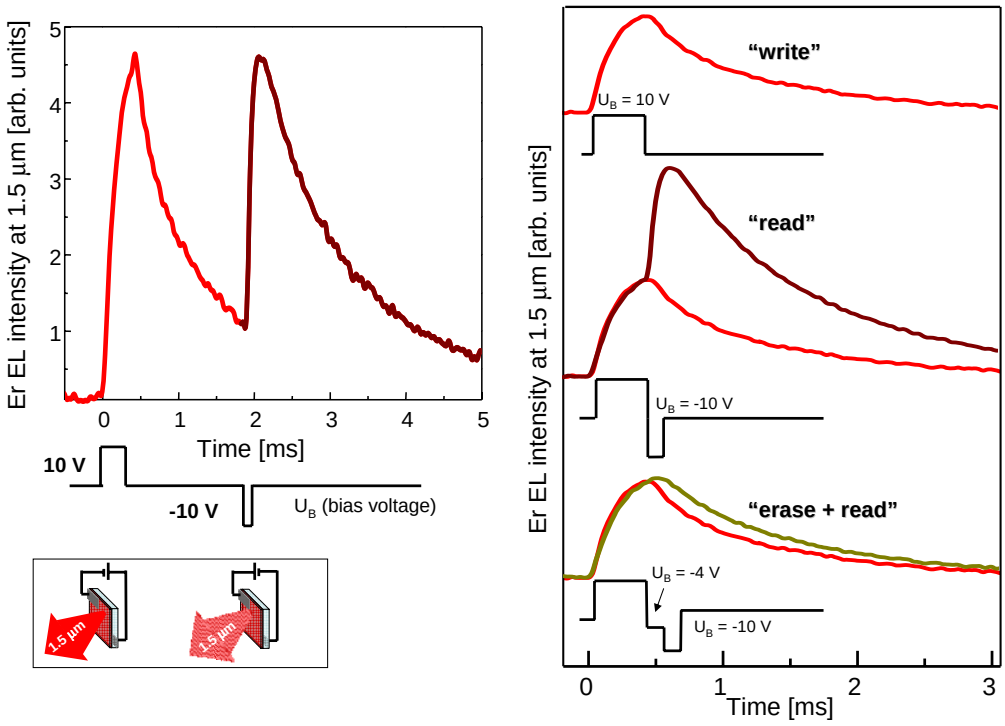

Figure 1.7: *Memory effect in electroluminescence observed at T = 77 K for the p-i-n structure investigated in the present study: information is written by a positive bias pulse, and subsequently read by a negative bias pulse of sufficiently large amplitude. (A negative bias pulse of sub threshold amplitude erases the information written with a positive bias.) The* write-read *and* write/erase-read *pulse sequences are shown. Note that the reverse bias of U_B = -10 V used for the* read *operation is considerably lower than the breakdown voltage.*

revealed that a long-term memory effect in EL under forward bias. Following a forward-bias pulse, additional emission—"stored" EL—from Er^{3+} ions could be induced by the application of a subsequent reverse bias pulse. This is illustrated in the left-hand panel of Fig. 1.7, where the EL response ($\lambda \approx 1.5$ μm) of the investigated structure is shown for a sequence of forward and reverse bias pulses, of $U_B = 10$ V, separated by a delay. It is important to note that the magnitude of the reverse bias pulse giving rise to this emission is well below the breakdown voltage, meaning that it cannot be due to EL resulting from avalanche breakdown of the reverse-biased p-n junction. Indeed, observation of the "stored" EL is possible only if the structure has been previously exposed to a forward bias pulse, thus representing a true memory function. Furthermore, a threshold dependence of the "stored" EL on the amplitude of the reverse-bias (*reading*) pulse has been found. A reverse-bias pulse of subthreshold magnitude, which did not induce emission, had an *erasing* effect, removing the *writing* effect of the initial pulse. This *write-erase-read* pulse sequence is also depicted on the right side in Fig. 1.7.

1.2.4 Discussion

Based on the available information, we propose the following microscopic mechanism for the observed EL memory effect: During the forward bias pulse, trapping centers available in the material are filled with carriers. This corresponds to the *write* operation, and can be accompanied by Er emission induced in a parallel process of electron-hole recombination. Under negative bias, the carriers localized in the traps are liberated into the band. If the electric field is higher than the threshold value (*e.g.* U_B = -10 V for the investigated structure), the carriers gain sufficient energy to excite Er^{3+} ions by impact. This is the *reading* process. A lower reverse bias (U_B = -4 V) removes the trapped carriers but does not provide enough energy for impact excitation; such a situation corresponds to *erasing*. This mechanism is schematically illustrated in Fig. 1.8, where it has been assumed that electrons are the carriers active in the process, since impact excitation of an Er^{3+} ion by electrons is known to be three orders of magnitude more efficient than by holes [46]. For the particular structure investigated here, the amplitude of the "stored" EL pulse was only slightly diminished when the delay time between the *write* and *read* pulses was set to 100 ms. This indicates a retention time of at least 0.5 s. As for thermal stability of the signal, very little signal deterioration was observed up to 120 K with the retention time being practically independent of temperature. This suggests that trapping centers responsible for the memory effect in the device are of deep rather than shallow character. Moreover, this moderate thermal quenching of signal intensity seems to be due to a less efficient filling of traps

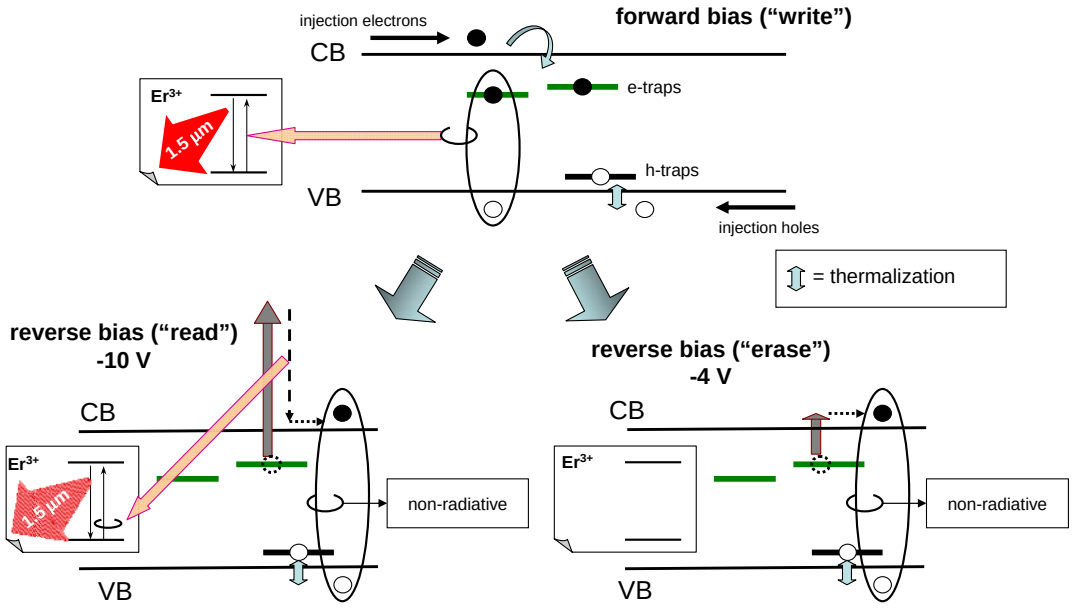

Figure 1.8: *Illustration of the proposed microscopic mechanism for the memory effect in electroluminescence. The positive bias pulse injects electrons and holes into the active layer in the depletion region. These fill traps available in the material. Parallel to that process, at higher injection rates, electron-hole recombination at specific Er-related centers may lead to excitation of Er^{3+} ions (initial emission pulse). The negative bias pulse liberates the (non-equilibrium) trapped carriers into the band; if its amplitude is sufficiently high, the carriers attain sufficient energy for impact excitation of Er.*

or to a less efficient excitation of Er at a higher temperature, rather than trap ionization. As mentioned before, these operational parameters of the future structures are very likely to be improved by the forthcoming investigations.

In current electronic technology, the storage hierarchy is governed by a compromise between density, access rate, and total data capacity as well as the cost of the individual memory element. For optical storage media, such as CD and DVD, the laser spot—currently of an order of 0.5 μm—limits the bit density. Furthermore, the access rate is determined by movement of mechanical parts that are required for precise beam positioning and, as such, represents a rather slow process. On the other hand, magnetic storage is currently reaching the physical limits of domain spacing as regards information density, and the spinning speed, with its access rate being, again, determined by mechanical movement of the *read/write* head. Semiconductor memories (DRAM, SRAM, ROM) are currently at the top of the storage hierarchy pyramid. These are basically transistors, which can be electrically programmed. While the development of transistors still follows Moore’s law [47], the cost of nanotooling increases exponentially with integration level, and thus it is generally acknowl-

edged that a further reduction of element size while maintaining a low-cost per element is likely to meet fundamental limitations already within the next few years.

The findings presented here indicate a possibility of using erbium-doped silicon for the development of future photonic memory devices. The investigated structure is the very first electrically operated Si:Er memory device to be fabricated and, as such, represents a "proof-of-principle". While its operational temperature and retention time are clearly not yet optimal, we believe that detailed understanding of the underlying physical mechanisms and consequent modification of material properties and device design can further improve these parameters. As the operating temperature range is enhanced, also the access rate will increase, as Er lifetime shortens and MHz signal modulation becomes possible [48]. Even higher rates should be feasible due to the fact that the device could be "reset" at a chosen clock frequency by an *erasing* pulse of reverse bias or by a flash of infrared laser light penetrating through the structure. In addition, massively parallel architectures might be used. A cartoon of a future Si:Er-based cross point memory array is shown in Fig. 1.9. The information is stored in active regions at the intersections of the "word" and "bit" lines. Similar to current flash memories, this array does not require any moving mechanical parts and individual elements are addressed by an appropriate choice of word and bit lines. By using vertical stacking and a 100 nm separation between lines, a hypothetical data density of up to 100 GB/cm^3 could be reached. This is comparable to values reached in prototypes of holographic memories [42], but in contrast to those, it does not require expensive laser systems. Nevertheless, it is only fair to point out, that intensity of individual light pulses emitted in the depicted structure during *read* operation would be very small, in view of a small number of Er ions contained in each memory element and non-radiative recombination increasing with temperature. Moreover, while the proposed concept is all-Si, the voltages of electrical pulses for *read* and *write* operations exceed those currently used in CMOS technology.

In addition to the storage applications, the memory function reported here might find an even more direct use in low-rate optical interconnects. Being, in fact, an all-silicon electro-optical converter operating at the 1.5 μm glass-fiber wavelength, it can provide an optical link between *e.g.* galvanically isolated parts of the system. The memory function could then be used for consecutive *writing* and parallel (packet) *reading* of information. Yet another highly speculative but exciting prospect, which could be explored, are spintronics applications, as the proposed device could, in principle, translate spin-polarization of electrons (in the electric pulses) into the polarization of emitted light—an effect which could be utilized in quantum computing schemes for spin read-out.

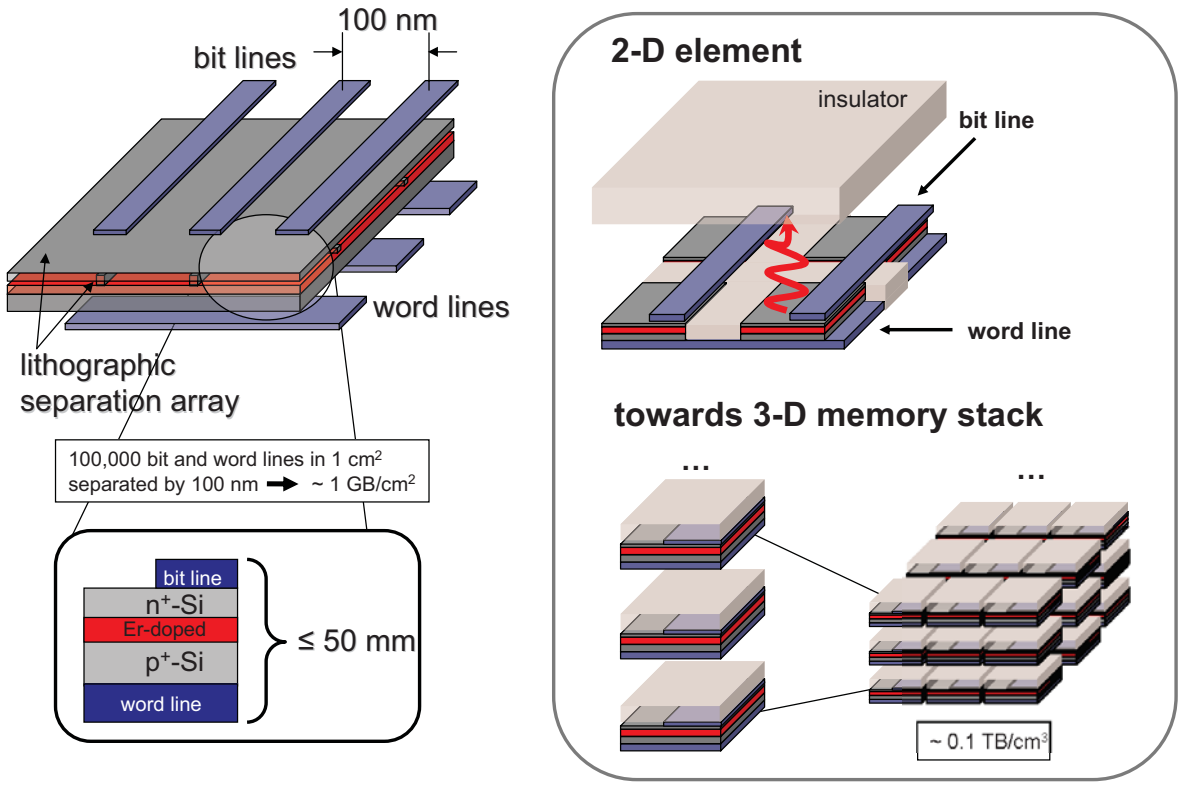

Figure 1.9: *A cartoon of an all-silicon photonic cross-memory array device based on the observed effect. The active layer is contained between crossed grids of bit and word lines; in that way an array of memory elements can be created. Similar to the current flash memories, each element can be individually addressed without any moving elements. Assuming a 100 nm repetition of line pattern, a density of* $\sim$ *1 GB/cm*^{2} *can be realized. Such "memory sheets" could be stacked vertically, resulting in a hypothetical volume density around 0.1 TB/cm*^{3}*.*

1.2.5 Conclusions

In summary, the presented here new functionality of c-Si:Er opens a route toward the ultimate goal of room-temperature photonic applications and on-chip-integrated optoelectronics. Coupled with advanced Si processing technology, this Si-based optoelectronic converter possessing true optical memory capability could be directly incorporated into nano-scale photonic circuits, enabling a new class of optoelectronic Si-based devices.